Journal of Alloys and Compounds 509 (2011) 9865–9868

Contents lists available at ScienceDirect

Journal of Alloys and Compounds

journal homepage: www.elsevier.com/locate/jallcom

Synthesis and upconversion luminescent properties of Er^{3+} doped and Er^{3+}–Yb^{3+} codoped GdOCl powders

Yong Li [a,*], Xiantao Wei [b], Min Yin [b]

[a] School of Mathematics and Physics, Anhui University of Technology, Maanshan 243000, China
[b] Department of Physics, University of Science and Technology of China, Hefei 230026, China

ARTICLE INFO

Article history:
Received 27 May 2011
Received in revised form 18 July 2011
Accepted 20 July 2011
Available online 27 July 2011

Keywords:
Phosphors
Solid state reaction
Upconversion
Luminescence

ABSTRACT

Er^{3+} doped and Er^{3+}–Yb^{3+} codoped GdOCl phosphors were prepared by modified solid state reaction. X-ray diffraction, scanning electron microscope, and Raman spectrum of the samples were studied. The result of Raman spectrum shows that the cutoff phonon energy of GdOCl is only 505 cm^{-1}, which is beneficial for upconversion luminescence. Infrared-to-visible upconversion emissions were observed under 980 nm diode laser excitation. It was found that the ratio of green to red upconversion emission intensity varies with concentration of the Er^{3+} or Yb^{3+} ion. Laser power and doping concentration dependence of upconversion luminescence were studied to understand the upconversion mechanisms. Excited state absorption and energy-transfer processes are proposed to be the possible mechanisms for the visible emissions.

1. Introduction

In the last few decades rare-earth doped upconversion luminescent materials have attracted great interest for their potential applications in many areas such as all-solid compact lasers, near-infrared quantum counting devices, optical data storage and fluorescent labels for sensitive detection of bimolecular [1–16]. Optical properties of trivalent lanthanide ions such as Er^{3+} in powders [1–5], crystals [17,18], ceramics [19–21] and glasses [16,22] in different host matrices have been extensively researched. Owing to low phonon energy and high upconversion efficiency [23,24], fluorides are the most widely investigated host materials for upconversion luminescence. However, the chemical stability and thermal stability of fluorides are poor. Besides, fluorides are usually difficult to be prepared. These factors are disadvantageous for the application. Oxide materials are another good choices for upconversion luminescence because of their relatively easier preparation and good physical and chemical stability [6,20], whereas the characteristic of oxides with higher phonon energy results in low upconversion efficiency. Therefore, it is an important challenge to find other hosts with good properties in this research field.

Lanthanum oxyhalides (LnOX, Ln = La, Y, Gd and X = F, Cl, Br) may combine the favorable properties from both the fluoride crystal and the oxide matrix. Having unique and excellent properties, they are good host matrixes for luminescence [10]. For example, Eu^{3+} and Tb^{3+} activated LaOBr phosphors have been widely used as X-ray intensifying phosphors [25,26]. In addition, their low phonon energy and chemical stabilities have turned them to be the most promising optical materials for upconversion phosphors in the recent years [27]. However, there are few reports about upconversion luminescence of rare earth ions doped LnOX. Gadolinium oxychloride (GdOCl) is one of the isomorphic series of LnOX. The GdOCl crystallizes in the tetragonal Matlockit-type PbFCl structure with *P4/nmm* space group. The crystal structure of GdOCl is comprised of alternating layers of the $(GdO)^+$ complex cations and the Cl^- anions. The Gd^{3+} cation is coordinated with four oxygens and five chlorines in a monocapped square antiprism arrangement with C_{4v} as the point symmetry of the Gd^{3+} site [28]. To the best of our knowledge, there are no reports about upconversion properties of rare-earth doped GdOCl. In the present work, Er^{3+} doped and Er^{3+}–Yb^{3+} codoped GdOCl powders were prepared by modified solid state reaction. Upconversion properties of GdOCl:Er^{3+} and GdOCl:Er^{3+},Yb^{3+} under 980 nm excitation have been investigated in detail for the first time, and the upconversion physical mechanism was discussed.

2. Experimental

The Er^{3+} doped or Er^{3+}–Yb^{3+} codoped GdOCl powders were prepared by modified solid state reaction. The starting materials are Gd_2O_3 (99.99%), Er_2O_3 (99.99%) and Yb_2O_3 (99.99%). Aqueous nitrate solutions were prepared by dissolving oxides in HNO_3 and distilled water under conditions of stirring and heating. The respective nitrate solutions with the required ratio were mixed. And then an excess of NH_4Cl was added to the mixed nitrate solution. The solution was stirred and dried. The dried precursor has been sintered in reducing atmospheres at 1000 °C for 0.5 h and 1 h, respectively. The GdOCl:Er^{3+} and GdOCl:Er^{3+},Yb^{3+} powders were obtained.

* Corresponding author. Tel.: +86 555 2315212.
E-mail address: yongli@ahut.edu.cn (Y. Li).

0925-8388/$ – see front matter © 2011 Elsevier B.V. All rights reserved.
doi:10.1016/j.jallcom.2011.07.060

The prepared samples appeared to be white color in body. It should be noted that the preparation method is different from conventional solid state reaction and wet chemical methods. Solid state reaction occurs between powders in the solid state, and it is comparatively simple and very suitable for mass production. While the wet chemical methods are usually based on chemical reactions, they offer the molecular-level mixing, the possibilities for controlling homogeneity and purity of phase. The modified solid state reaction described above has the advantages of both preparation methods. It offers the molecular-level mixing in the first stage of the preparation process, and occurs eventually between powders in solid state.

X-ray diffraction (XRD) studies were carried out on the powders for phase identification by using a rotating anode X-ray diffractometer (MAC Science Co. Ltd., MXP18AHF) under Cu K_α radiation. The morphological features of the powders were examined by a Field emission Scan Electron Microanalyzer (FESEM, Model JSM-6700F, JEOL, Japan). Raman spectrum was measured by a LABRAM-HR laser Raman spectrometer. An Ar-ion laser with a wavelength of 514.5 nm was used as the light resource for Raman study. The upconversion emissions excited by a 980 nm diode laser were dispersed by a Jobin-Yvon HRD-1 monochromator and detected by Hamamatsu R928 photomultiplier. The signal was analyzed by an EG&G 7625 DSP lock-in amplifier and stored into computer memories. All the spectra were measured at room temperature.

3. Results and discussion

XRD pattern of the GdOCl phosphors prepared by modified solid state reaction is shown in Fig. 1. The diffraction pattern of samples prepared at 1000 °C for 0.5 h almost matches that of GdOCl crystalline (JCPDS 85-1199). Trace of Gd_2O_3 appears as a secondary product of the synthesis (corresponding weak diffraction peak marked with asterisk). The diffraction peak of Gd_2O_3 disappears in the sample prepared at 1000 °C for 1 h. It can be seen that the intensity of diffraction peak increases and half width of diffraction peak decreases with the time required for sample preparation, which indicates the increase of GdOCl crystallite size. The morphology and size of the powders were characterized by using scanning electron microscope (SEM) as shown in Fig. 2. The GdOCl product synthesized at 1000 °C for 1 h shows smooth plate-like particles with various diameters from 100 nm to 2 μm, and there is a small amount of agglomeration in the particles. The XRD patterns and SEM observation of samples doped with Er^{3+}, Yb^{3+} ions were also characterized, revealing that the introduction of the activator does not influence the crystal structure and morphology of the phosphor matrix. It is well known that upconversion efficiency will be suppressed by the multiphonon relaxation of the metastable energy level. Phosphors with low phonon energies would decrease the multiphonon relaxation and have high upconversion efficiency. Here Raman spectroscopy was used to characterize the phonon vibrational frequency of GdOCl. As shown in Fig. 3, the Raman spectrum of GdOCl shows five of the six possible lines corresponding to the modes with the irreducible representations $2A_{1g} + 3E_g + B_{1g}$,

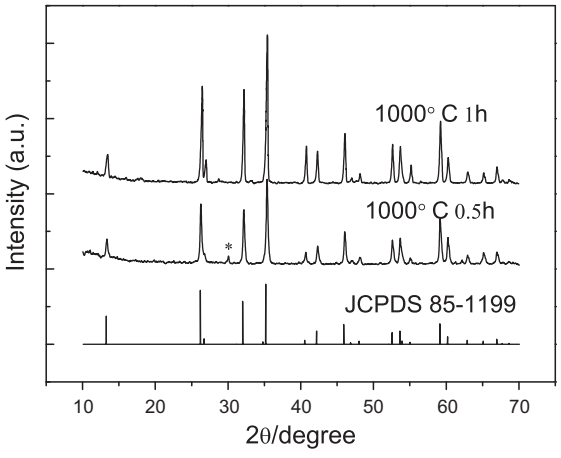

Fig. 1. XRD patterns of GdOCl powders prepared at 1000 °C with different holding time.

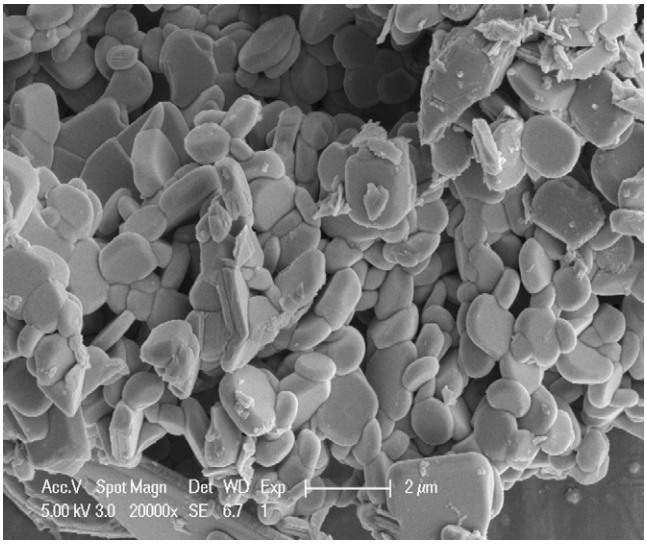

Fig. 2. SEM image of GdOCl powders prepared at 1000 °C for 1 h.

The five intense peaks at 118 cm^{-1}, 181 cm^{-1}, 235 cm^{-1}, 376 cm^{-1}, and 505 cm^{-1} are fair agreement with the previous report in reference [29], which also confirms the tetragonal Matlockit-type PbFCl structure of the sample. Moreover, as can be seen from Fig. 3, the phonon cutoff energy of GdOCl is only about 505 cm^{-1}, which is lower than that of Gd_2O_3 (about 570 cm^{-1}) [6] and Y_2O_3 (about 600 cm^{-1}) [2], therefore GdOCl is supposed to be a good host material for upconversion.

Visible upconversion emission of GdOCl doped with different Er^{3+} ion concentration under excitation of 980 nm diode laser is presented in Fig. 4. The upconversion emission spectra consist of intense green emission bands centered at 550 nm along with a group of relatively weak emission bands in the 650–680 nm regions. The green bands are ascribed to the intra 4f–4f electronic transitions $^2H_{11/2}$, $^4S_{3/2} \rightarrow {}^4I_{15/2}$ of Er^{3+} ion, while the red band is assigned to $^4F_{9/2} \rightarrow {}^4I_{15/2}$ transition. It is clear from Fig. 4 that the emission intensities and the energy distribution of the upconverted emission spectra depend on Er^{3+} ion concentration. The emission intensity is the strongest in 8 mol% Er^{3+} doped powders and decreases when the doping concentration of Er^{3+} reaches 12 mol%. The ratio of red to green emission intensity increases with Er^{3+} concentration. As the Er^{3+} concentration increases from 1 to 12 mol%, the ratios are around 0, 0.1, 0.4 and 0.5, respectively. As shown in Fig. 5 the general features of upconversion spectra of GdOCl:Er^{3+}1% powders with different Yb^{3+} ion concentration are similar to those

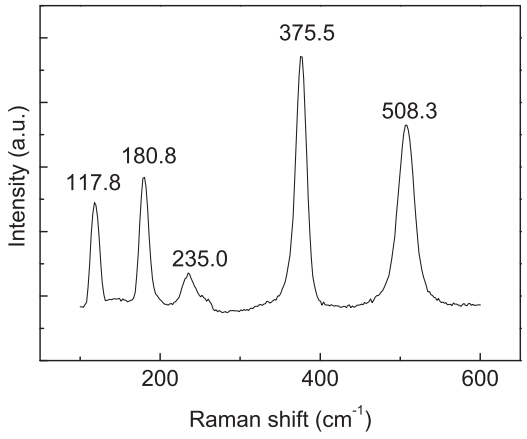

Fig. 3. Raman spectrum of pure GdOCl sample.

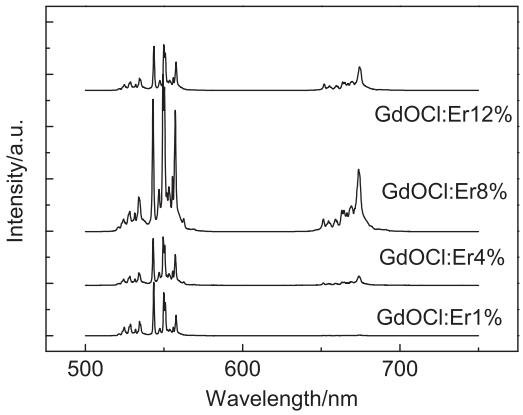

Fig. 4. Upconversion spectra of Er^{3+} doped GdOCl powders with different Er^{3+} concentration.

observed in Er^{3+} singly doped GdOCl powders. The green and red bands also correspond to the intra 4f–4f electronic transitions of Er^{3+} ion. It should be noted that intensities of the emission bands are significantly higher than that observed in Er^{3+} singly doped samples. For the sample with low content (1–4 mol%) of Yb^{3+}, the green emission is dominant; while at the high doping level, the green emission tends to trail off, and the red one is dominant in the spectra. The ratio of red to green emission intensity also increases with Yb^{3+} concentration. Such a result is also observed from Er^{3+} doped and Er^{3+}–Yb^{3+} codoped in other host matrices [2,19]. The concentration dependence of upconversion emissions could be mainly attributed to the interactions between doping ions.

To understand better the physical mechanisms which are responsible for the upconversion luminescence described above, the emission intensities were measured as a function of the pumping power. It is well known that the upconverted emission intensity (I_{em}) depends on the pumping laser power (I_{pump}) according to the equation: $I_{em} \sim I_{pump}^{n}$, where n is the number of pumping photons absorbed per upconverted photon emitted. The logarithmic plot of the upconversion emission intensities as a function of the pumping laser power is shown in Fig. 6. The plot of ln I_{em} versus ln I_{pump} yields a straight line. The obtained n was 1.71 ± 0.06, 1.73 ± 0.06 and 1.67 ± 0.06 for 534 nm ($^2H_{11/2} \rightarrow {}^4I_{15/2}$), 549 nm ($^4S_{3/2} \rightarrow {}^4I_{15/2}$) and 674 nm ($^4F_{9/2} \rightarrow {}^4I_{15/2}$) emissions in 12 mol% Er^{3+} doped GdOCl powders, respectively. While in the sample of GdOCl:Er^{3+}1%Yb^{3+}4%, the slope n was 1.97 ± 0.14, 1.99 ± 0.16 and 1.86 ± 0.06 for green ($^4S_{3/2} \rightarrow {}^4I_{15/2}$, $^2H_{11/2} \rightarrow {}^4I_{15/2}$) and red ($^4F_{9/2} \rightarrow {}^4I_{15/2}$) emissions respectively. These results indicate that the two-photon process is responsible for the red and green upconversions.

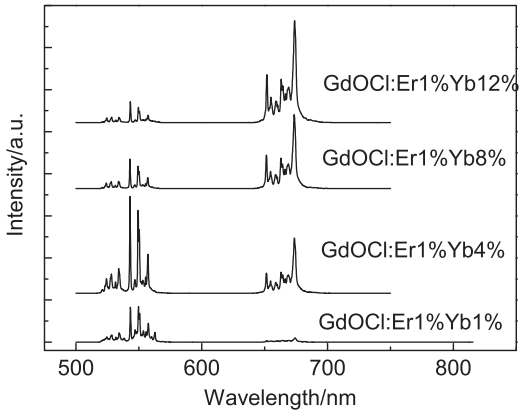

Fig. 5. Upconversion spectra of Er^{3+}–Yb^{3+} codoped GdOCl powders with different Yb^{3+} concentration.

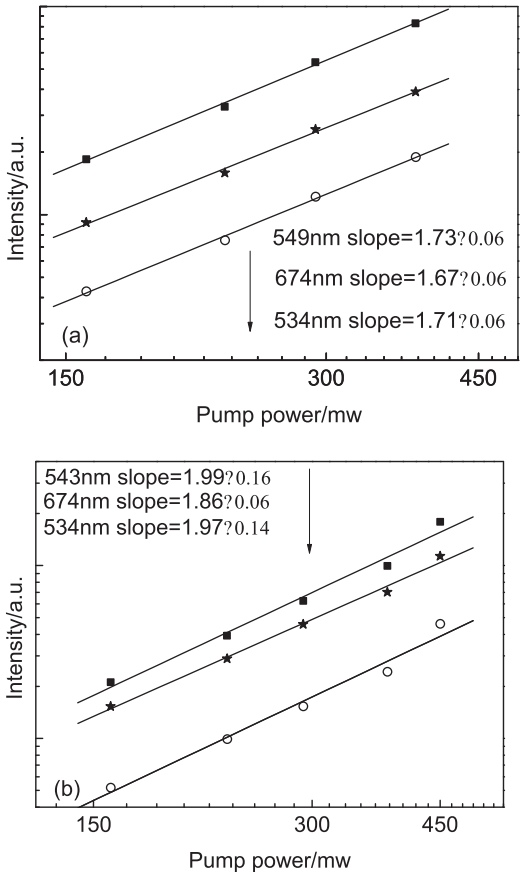

Fig. 6. Pump power dependence of upconversion emission in different samples. (a) GdOCl:Er^{3+}12%; (b) GdOCl:Er^{3+}1%Yb^{3+}4%.

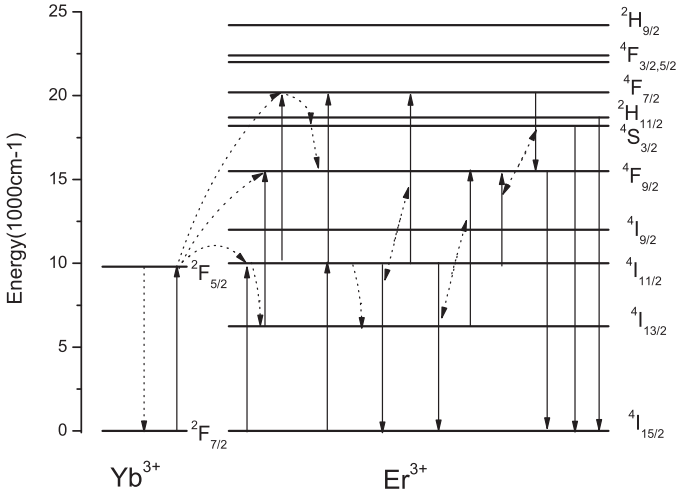

Fig. 7. Energy level diagrams of Er^{3+} and Yb^{3+} in GdOCl matrix and the proposed upconversion mechanism.

Fig. 7 gives the energy level diagram of Er^{3+} and Yb^{3+} ions and the probable upconversion mechanisms. For Er^{3+} singly doped samples, Er^{3+} ions are excited from the ground state to the $^4I_{11/2}$ state by ground state absorption. Another 980 nm photon excites the same ion to the $^4F_{7/2}$ state. This is an excited-state absorption (ESA) process. Multi-phonon relaxation from the $^4F_{7/2}$ state is responsible for populating the $^2H_{11/2}$ and $^4S_{3/2}$ states, and the green emissions are yielded through the transitions of $^4S_{3/2} \rightarrow {}^4I_{15/2}$, $^2H_{11/2} \rightarrow {}^4I_{15/2}$. There is another possible energy transfer (ET) route that can also

populate the $^4F_{7/2}$ state: $2^4I_{11/2} \rightarrow {}^4F_{7/2} + {}^4I_{15/2}$. In this process, an excited Er^{3+} ion will relax from $^4I_{11/2}$ state to $^4I_{15/2}$ state nonradiatively by transferring its energy to a neighboring ion in the same state, promoting the latter one to $^4F_{7/2}$ state. ESA would be the most likely mechanism in samples with low doping concentration as the doping ions are too far apart to interact with each other. However, as the doping concentration is increased, the probability of ET also increases. The luminescent $^4F_{9/2}$ level can be pumped via a nonradiative relaxation through the $^4S_{3/2}$ excited state. Taking the change of relative intensity of red and green emissions in the samples with different Er^{3+} concentrations into account, it is reasonable to assume that there must be other processes that only populate the $^4F_{9/2}$ state. The first process suggested to explain the increase of red emission intensity with Er^{3+} concentration is resonant cross relaxation mechanism proposed by Fiorenzo: $^4F_{7/2} + {}^4I_{11/2} \rightarrow 2^4F_{9/2}$ [30]. This cross relaxation process is only efficient in high doping concentration. Another possible process is a cross-relaxation process between two neighboring Er^{3+} ions described as follows: $^4I_{13/2} + {}^4I_{11/2} \rightarrow {}^4F_{9/2} + {}^4I_{15/2}$. The energy gap between $^4I_{13/2}$ and $^4I_{11/2}$ is approximately 3600 cm^{-1}, it require approximately seven intrinsic GdOCl phonons to bridge, which make multiphonon relaxation nearly impossible. However, the CO_3^{2-} and OH^- could be introduced during sample preparation, whose vibrational energies are about 1500 and 3350 cm^{-1}, respectively [20]. And the $^4I_{13/2}$ level can be populated through a multiphonon nonradiative process from the $^4I_{11/2}$ state, which utilizes these high energy phonons. It should be pointed out that the former process is dominant in samples with high doping levels.

For Er^{3+}–Yb^{3+} codoped samples, an Er^{3+} ion can be excited from the ground state to $^4I_{11/2}$ level by ground state absorption and energy transfer from excited Yb^{3+} ions. This energy transfer process can be described as $^4I_{15/2}$ (Er) + $^2F_{5/2}$ (Yb) → $^4I_{11/2}$ (Er) + $^2F_{7/2}$ (Yb). The later process is the dominant one, confirmed by the great increase of upconversion emission intensity in the codoping samples. The populated $^4I_{11/2}$ state can be excited to the $^4F_{7/2}$ by three processes: excited state absorption (ESA), energy transfer between Er^{3+} ions described above, and energy transfer from excited Yb^{3+} ion to the $^4I_{11/2}$ state of Er^{3+} ion described as follows: $^4I_{11/2}$ (Er) + $^2F_{5/2}$ (Yb) → $^4F_{7/2}$ (Er) + $^2F_{7/2}$ (Yb). The populated $^4F_{7/2}$ state of Er^{3+} then relaxes rapidly and nonradiatively to the next lower $^2H_{11/2}$ and $^4S_{3/2}$ luminescent state. Taking consideration on luminescence behaviors, the red emissions intensity and the ratio of red to green emissions intensity have been gradually enhanced with the increase of concentration of Yb^{3+}. The $^4F_{9/2}$ state can also be populated by the processes described in Er^{3+} singly doped samples which are inefficient when the Er^{3+} doping concentration is low. In addition, there is another important energy transfer process in Er^{3+}–Yb^{3+} codoped samples. It can be described as follows: $^4I_{13/2}$ (Er) + $^2F_{5/2}$ (Yb) → $^4F_{9/2}$ (Er) + $^2F_{7/2}$ (Yb). In this mechanism, an excited Yb^{3+} ion will relax from $^2F_{5/2}$ state to $^2F_{7/2}$ state nonradiatively by transferring its energy to a neighboring Er^{3+} ion in the $^4I_{13/2}$ state, promoting the latter one to $^4F_{9/2}$ state. Obviously, the energy transfer efficiency between Yb^{3+} and Er^{3+} ions depends on the concentration of Yb^{3+} and Er^{3+} ions. At high Yb^{3+} ions concentration, this process is very efficient and results in red emission enhancement. It should be noted that the energy transfer process from Yb^{3+} to Er^{3+} ions is dominant because of the low Er^{3+} doping concentration (1 mol%) and the much larger absorption cross-section of Yb^{3+} ions around 980 nm. When the Yb^{3+} doping concentration achieves to 12 mol%, concentration quenching occurs, and the intensities of all the upconversion emission bands decrease.

4. Conclusions

In summary, Er^{3+} doped and Er^{3+}–Yb^{3+} codoped GdOCl samples have been prepared by modified solid state reaction. Visible upconversion emission of the samples under 980 nm laser excitation is reported and discussed. The Er^{3+} or Yb^{3+} concentration has significant influence on the energy distribution of upconversion spectra. Excited state absorption and energy transfer processes are the possible mechanisms of this behavior. Power dependence analysis reveals that the green and red emissions originate from a two-photon upconversion process.

Acknowledgements

This work was supported by National Nature Science Foundation of China (50903001, 10774140, 11074245, and 11011120083), China Postdoctoral Science Foundation (20100480693), Knowledge Innovation Project of The Chinese Academy of Sciences (KJCX2-YW-M11), Special Foundation for Talents of Anhui Province, China (2007Z021).

References

[1] I.I. Leonidov, V.G. Zubkov, A.P. Tyutyunnik, N.V. Tarakina, L.L. Surat, O.V. Koryakova, E.G. Vovkotrub, J. Alloys Compd. 509 (2011) 1339–1346.
[2] G.Y. Chen, Y. Liu, Y.G. Zhang, G. Somesfalean, Z.G. Zhang, Q. Sun, F.P. Wang, Appl. Phys. Lett. 91 (2007) 133103.
[3] H. Ping, D. Chen, Y. Yu, Y. Wang, J. Alloys Compd. 490 (2010) 74–77.
[4] G. Chen, G. Somesfalean, Y. Liu, Z. Zhang, Q. Sun, F. Wang, Phys. Rev. B 75 (2007).
[5] A. Patra, C.S. Friend, R. Kapoor, P.N. Prasad, Chem. Mater. 15 (2003) 3650–3655.
[6] H. Guo, N. Dong, M. Yin, W. Zhang, L. Lou, S. Xia, J. Phys. Chem. B 108 (2004) 19205–19209.
[7] A. Shalav, B.S. Richards, T. Trupke, K.W. Krämer, H.U. Güdel, Appl. Phys. Lett. 86 (2005) 013505.
[8] J.A. Capobianco, J.C. Boyer, F. Vetrone, A. Speghini, M. Bettinelli, Chem. Mater. 14 (2002) 2915–2921.
[9] D. Chen, Y. Wang, Y. Yu, P. Huang, Appl. Phys. Lett. 91 (2007) 051920.
[10] D. Chen, Y. Wang, K. Zheng, T. Guo, Y. Yu, P. Huang, Appl. Phys. Lett. 91 (2007) 251903.
[11] D. Chen, Y. Yu, P. Huang, F. Weng, H. Lin, Y. Wang, Appl. Phys. Lett. 94 (2009) 041909.
[12] D. Chen, Y. Yu, F. Huang, P. Huang, A. Yang, Y. Wang, J. Am. Chem. Soc. 132 (2010) 9976–9978.
[13] D. Chen, P. Huang, Y. Yu, F. Huang, A. Yang, Y. Wang, Chem. Commun. 47 (2011) 5801–5803.
[14] D. Chen, Y. Yu, F. Huang, Y. Wang, Chem. Commun. 47 (2011) 2601–2603.
[15] D. Chen, Y. Yu, F. Huang, A. Yang, Y. Wang, J. Mater. Chem. 21 (2011) 6186.
[16] J. Ding, Q. Zhang, J. Cheng, X. Liu, G. Lin, J. Qiu, D. Chen, J. Alloys Compd. 495 (2010) 205–208.
[17] T. Hebert, R. Wannemacher, W. Lenth, R.M. Macfarlane, Appl. Phys. Lett. 57 (1990) 1727–1729.
[18] L. Li, Z. Zhou, L. Feng, H. Li, Y. Wu, J. Alloys Compd. 509 (2011) 6457–6461.
[19] G. Qin, J. Lu, J. Bisson, Y. Feng, K. Ueda, H. Yagi, T. Yanagitani, Solid State Commun. 132 (2004) 103–106.
[20] J. Zhang, S. Wang, L. An, M. Liu, L. Chen, J. Lumin. 122–123 (2007) 8–10.
[21] X. Hou, S. Zhou, T. Jia, H. Lin, H. Teng, J. Alloys Compd. 509 (2011) 2793–2796.
[22] G.S. Maciel, C.B. Araújo, Y. Messaddeq, M.A. Aegerter, Phys. Rev. B 55 (1997) 6335.
[23] S. Tanabe, H. Hayashi, T. Hanada, N. Onodera, Opt. Mater. 19 (2002) 343–349.
[24] Z. Li, L. Zheng, L. Zhang, L. Xiong, J. Lumin. 126 (2007) 481–486.
[25] K.R. Reddy, V. Aruna, T. Balaji, K. Annapuma, S. Buddhudu, Mater. Chem. Phys. 52 (1998) 157–160.
[26] J. Yang, J. Gong, H. Fan, L. Yang, J. Mater. Sci. 40 (2005) 3725–3728.
[27] H. Guo, Opt. Mater. 29 (2007) 1840–1843.
[28] S.-S. Lee, H.-I. Park, C.-H. Joh, S.-H. Byeon, J. Solid State Chem. 180 (2007) 3529–3534.
[29] S. Areva, J. Hölsä, R.-J. Lamminmäki, H. Rahiala, P. Deren, W. Strek, J. Alloys Compd. 300–301 (2000) 218–223.
[30] F. Vetrone, J.-C. Boyer, J.A. Capobianco, A. Speghini, M. Bettinelli, Chem. Mater. 15 (2003) 2737–2743.